Color discrimination in anomalous trichromacy: experiment and theory

Article (Published Version)

Vision Research 188 (2021) 85–95

Contents lists available at ScienceDirect

Vision Research

journal homepage: www.elsevier.com/locate/visres

Color discrimination in anomalous trichromacy: Experiment and theory

Alexandra E. Boehm [a,b,c,*], Jenny Bosten [a,d], Donald I.A. MacLeod [a]

[a] Department of Psychology, University of California, San Diego, CA, USA
[b] Vision Science Graduate Group, University of California, Berkeley, CA, USA
[c] School of Optometry, University of California, Berkeley, CA, USA
[d] School of Psychology, University of Sussex, Brighton, UK

ARTICLE INFO

Keywords:
Anomalous trichromacy
Deuteranomaly
Protanomaly
Color vision deficiency
Color vision
Chromatic contrast
Color discrimination
Post-receptoral compensation

ABSTRACT

In anomalous trichromacy, the color signals available from comparing the activities of the two classes of cone sensitive in the medium and long wavelength parts of the spectrum are much reduced from those available in normal trichromacy, and color discrimination thresholds along the red-green axis are correspondingly elevated. Yet there is evidence that suprathreshold color perception is relatively preserved; this has led to the suggestion that anomalous trichromats post-receptorally amplify their impoverished red-green signals. To test this idea, we measured chromatic discrimination from white and from saturated red and green pedestals. If there is no post-receptoral compensation, the anomalous trichromat's loss of chromatic contrast will apply equally to the pedestal and to the test color. Coupled with a compressively nonlinear neural representation of saturation, this means that a given pedestal contrast will cause a smaller than normal modulation of discrimination sensitivity. We examined cases where chromatic pedestals impair the color discrimination of normal trichromatic observers. As predicted, anomalous observers experienced less impairment than normal trichromats, though they remained less sensitive than normal trichromats. Although the effectiveness of chromatic pedestals in impairing color discrimination was less for anomalous than for normal trichromats, the chromatic pedestals were more effective for anomalous observers than would be expected if the anomalous post-receptoral visual system were the same as in normal trichromacy; the hypothesis of zero compensation can be rejected. This might suggest that the effective contrast of the pedestal is post-receptorally amplified. But on closer analysis, the results do not support candidate simple models involving post-receptoral compensation either.

1. Introduction

In normal trichromatic color vision there are three types of cone photoreceptors, distinct in their sensitivities to short (S), medium (M), and long (L) wavelengths of light. Comparisons of the signals arising from S, M and L cones by the post-receptoral visual system underlie the discrimination of color.

Anomalous trichromacy is a congenital color vision deficiency where, as in normal color vision, there are three classes of cone, but the spectral sensitivity of the anomalous cone photopigment is different from the norm. Approximately 6% of human males have deuteranomaly or protanomaly, which is the result of an alteration in spectral sensitivity of the M or L cones. Because the genes for the M and L cone photopigments are located adjacently on the X-chromosome and have similar sequences, hybrid genes resulting in anomalous photopigments are not uncommon, with the separation of the peak spectral sensitivities of the M and L cones typically varying from as little as 1 nm to as much as 12 nm (Merbs & Nathans, 1992).

In anomalous trichromacy, the two cone types that are sensitive to medium and long wavelengths of light are more similar in their spectral sensitivities than are the normal M and L cones. In deuteranomaly, the normal M cone is replaced by an anomalous cone with a spectral sensitivity close to that of the normal L cone, that we refer to as L'. Similarly, in protanomaly, M' cones, with a spectral sensitivity close to that of the normal M cones, replace the L cones. For both protanomals and deuteranomals, the greater spectral overlap between the sensitivities of the two cone types sensitive at medium and long wavelengths effectively reduces chromatic contrast in the corresponding region of the visible spectrum. Consequently, color discrimination is impaired (e.g. Pokorny, Smith, Verriest, & Pinckers, 1979; Rodriguez-Carmona & Barbur, 2012).

The post-receptoral representation of color in anomalous trichromacy depends on both the spectral sensitivities of the cones and the function of post-receptoral neural pathways. If the post-receptoral

* Corresponding author.

https://doi.org/10.1016/j.visres.2021.05.011
Received 30 August 2020; Received in revised form 28 May 2021; Accepted 29 May 2021
Available online 20 July 2021

pathways are the same as in normal color vision, what we refer to as 'zero compensation', the "red-green" opponent system would be understimulated and would not make use of the full neural capacity that is available (MacLeod, 2003). In principle, though, this loss of signal strength could be avoided by a post-receptoral *neural compensation*. Regan and Mollon (1997) and others (MacLeod, 2003; Bosten, Robinson, Jordan, & Mollon, 2005; Webster, Juricevic, & McDermott, 2010; Boehm, MacLeod, & Bosten, 2014) have suggested that the visual systems of anomalous trichromats might post-receptorally amplify the reduced cone opponent signals (see Barbur et al., 2008 for a related hypothesis that cone-specific post-receptoral amplification may compensate for differences in the ratio of L to M cone numbers). This adaptive range adjustment could allow the weakened color signals that arise from comparing the activities of the cone types present in anomalous trichromacy to span the full normal range of post-receptoral signals.

We have investigated how the color discrimination of anomalous observers is affected when the compared fields are separate and clearly distinguished from their common background (the pedestal case). We ask: are the results consistent with the simple hypothesis that anomalous and normal trichromats have identical post-receptoral neural organization (zero compensation)? Or do they support the competing hypothesis that the initially impoverished chromatic signals in the anomalous trichromatic retina undergo a compensatory post-receptoral enhancement? Anomalous trichromacy is here exploited as a natural developmental experiment. Is the color vision system plastic enough to allow a potentially beneficial change in post-receptoral organization in response to altered inputs, or is the organization fixed in a design shared between observers with normal and anomalous cone pigments?

Four existing studies provide evidence for neural compensation in anomalous trichromats. First, Regan and Mollon (1997) measured the relative saliences of chromatic patterns that varied along the two cardinal axes of the MacLeod-Boynton (1979) chromaticity diagram, L/(L + M) and S/(L + M). They found that despite the reduced contrast between the activities of the cones sensitive to long and medium wavelengths, for some anomalous trichromats the relative salience of chromatic variation along the L/(L + M) axis (compared to variation along the S/(L + M) axis) was the same as for normal trichromats.

Second, we (Boehm et al., 2014) have compared the performance of anomalous trichromats at threshold with their suprathreshold perception of color. We measured thresholds for chromatic discrimination from white along the cardinal axes of the MacLeod-Boynton chromaticity diagram (S/(L + M) and L/(L + M)). We then compared the ratio of the two thresholds with the ratio of variation in color appearance along the same axes in a color space reconstructed using multidimensional scaling (MDS). We found that although for anomalous trichromats sensitivity for detecting differences in L/(L + M) was only 19%-38% of that of normal trichromats, their MDS-reconstructed suprathreshold color space spanned 67%-86% of the normal range along the same axis.

More recently, Knoblauch, Marsh-Armstrong, and Werner (2020) used maximum likelihood difference scaling to compare suprathreshold contrast appearance for anomalous and normal trichromats. Participants viewed Gabor patterns modulated in L/(L + M) contrast and judged which of two stimuli appeared most similar to a reference stimulus that varied in achromatic (luminance) contrast. They found that while anomalous observers required higher L/(L + M) contrasts for detection, the magnitude of perceived suprathreshold L/(L + M) contrasts (with increasing physical (L/(L + M) contrast) increased more rapidly for anomalous trichromats than for normal trichromats, a result that could not be explained by a simple model where the effective chromatic contrast is reduced due to the greater spectral overlap of their cone pigments.

Tregillus et al. (2021) have provided neuroimaging evidence for post-receptoral compensation in anomalous trichromacy. In response to gratings modulated along S/(L + M) and L/(L + M) in both normal and anomalous trichromats, they found that BOLD responses to L/(L + M) gratings were of the same amplitude in the two groups in areas V2 and V3, but much reduced in anomalous trichromats in V1. Their results imply that there is post-receptoral compensation in the cortical representation of L/(L + M) contrast for anomalous trichromats, but that this occurs after V1.

These findings suggest that once a red-green color difference is large enough to be easily detected by an anomalous observer, it appears to them with nearly normal vividness. This could readily be explained by a neural compensation process of the sort described above. We here use color discrimination as a test of the neural compensation hypothesis. In normal trichromacy, color discrimination is limited, at least in part, by the compressively nonlinear contrast response functions of post-receptoral neurons. Following Birdsall's theorem (Lasley & Cohn, 1981) a compressively nonlinear transformation of the sensory input must precede the site where the dominant source of noise that limits performance is introduced in order to affect discrimination (otherwise, signal to noise comparisons before and after the nonlinearity would be identical). When driven by high contrast stimuli, for example by chromatic pedestals, compression reduces the slope of contrast response functions, leading to smaller differences between signals. The introduction of noise after the site of compression makes these reduced differences in some cases indiscriminable, elevating thresholds. An anomalous observer, without post-receptoral compensation, might evade the loss of sensitivity if their reduced chromatic contrast signals are restricted to the lower end of the post-receptoral neurons' range of contrast response. Alternatively, if their signals are post-receptorally amplified to span the full normal range, then the effects of the compression on discrimination thresholds would be apparent in their discrimination performance as it is in normal trichromacy.

In normal trichromacy color discrimination is markedly impaired when measured with saturated pedestals that contain chromatic contrast relative to the background, so that a plot of discrimination threshold against pedestal chromaticity traces out a V profile, with minimum threshold (indicating best discrimination) for pedestals that are not different in color from the background (see for instance, Krauskopf & Karl, 1992; Miyahara, Smith, & Pokorny, 1993; Vingrys & Mahon, 1998; Watanabe, Pokorny, & Smith, 1998; Smith, Pokorny, & Sun, 2000; Chen, Foley, & Brainard, 2000; Kawamoto, Inamura, Yaguchi, & Shioiri, 2003; or Fig. 2). The V profile is expected if noise originates in contrast sensitive neurons, whose incremental sensitivity is compromised when they are driven hard by the pedestal (see for instance Pugh & Mollon, 1979; von der Twer & MacLeod, 2001; MacLeod & von der Twer, 2003). The compressive nonlinearity in chromatic contrast response functions revealed psychophysically has also been demonstrated by physiological measurements of macaque retina (Lee, Pokorny, Martin, Valbergt, & Smith, 1990; Yeh, Lee, & Kremers, 1995). However, the physiological data do not typically show such a severe compression as psychophysical data (MacLeod, 2003), and some physiologists find a nearly linear relationship (Blessing, Solomon, Hasheimi-Nedhad, Morris, & Martin, 2004). A stronger compressive nonlinearity in response to isoluminant chromatic contrast has been shown in macaque V4 cells (Bushnell, Harding, Kosai, Bair, & Pasupathy, 2011), perhaps indicating that the compressive nonlinearity revealed psychophysically may arise downstream of the retina. Additionally, evidence from neuroimaging shows a compressive nonlinearity in the representation of chromatic contrast (EEG: Di Russo, Spinelli, and Morrone (2001), GOMES et al. (2006), Souza et al. (2008), Kaneko, Kuriki, and Andersen (2020), fMRI: Tregillus et al. (2021)).

In the present study, participants viewed four colored patches presented against an achromatic background. The four colored patches may be regarded as chromatic pedestals, with a small color difference applied to the test patch making it of higher saturation than the other three patches. Participants were asked to identify the most saturated of the four patches. The saturation of the pedestals varied across conditions: they could be achromatic (hence with no chromatic contrast), green or red. Our objective was to determine whether anomalous observers

experience a similar impairment of discrimination by saturated pedestals, and whether their discrimination performance supports the hypothesis of post-receptoral neural compensation (see Lutze, Pokorny, and Smith (2006) for a related hypothesis about achromatic contrast discrimination in people with color vision deficiency).

The simplest possible scenario that we consider for the relation between normal and anomalous trichromats is that the post-receptoral organization of the visual system of anomalous observers is completely normal, without any neural compensation to remedy the deficit associated with the pigment swap (different photopigments from those of normal trichromats). On this Zero Compensation model, the anomalous trichromat's pigment swap reduces the effective chromatic contrast signaled by long- and middle-wave sensitive cones by the same factor for pedestal and test stimuli alike. A pedestal with high chromatic contrast that saturates a color contrast encoding neuron in the normal trichromat may therefore fail to saturate it in the anomalous observer. For the anomalous observer, therefore, the pedestal-evoked increases in discrimination threshold expressed in the V profile will be reduced, and the V slope will be made correspondingly shallower. The discrimination deficit associated with anomalous trichromacy will accordingly be reduced, or—intriguingly—perhaps even disappear or be reversed, when discrimination is assessed on red or green pedestals.

The precise forms of the functions relating saturation increment threshold to pedestal saturation depend on (i) the presence, absence or degree of post-receptoral compensation, but also on (ii) whether the neural noise that limits performance occurs early, before the compressive nonlinearity in the representation of saturation and before post-receptoral compensation, or late, after the compressive nonlinearity and post-receptoral compensation. We incorporate these different considerations into various models (see "Models") that predict the different forms of the "V" curves given these different considerations, and consider these predictions in relation to the results.

2. Methods

2.1. Participants

Participants were 7 normal trichromats, 5 deuteranomals, and 2 protanomals. All participants with abnormal color vision were males. Of those with normal color vision, 4 were males and 3 were females. Normal color vision was confirmed with an anomaloscope.

Anomalous participants were recruited following screening using an anomaloscope of approximately 350 undergraduate students at the University of California, San Diego. Extreme anomalous trichromats (where the matching range includes the normal match) were excluded. The anomalous participants that participated in this study also participated in the experiments of Boehm et al. (2014). All participants were undergraduate volunteers at UC San Diego or lab members. Volunteers were compensated at a rate of ten dollars per hour. Participants gave written informed consent for their participation. The study was approved by the UC San Diego Human Research Protections IRB and adhered to the principles of the Declaration of Helsinki at the time the study was conducted.

3. Equipment

The anomaloscope was a two-channel optical system. Participants matched two halves of a bipartite field by adjusting the relative mixture of red and green primaries presented on a DreamColor LP2480ZX (Hewlett Packard, Palo Alto, CA) until it appeared identical to a monochromatic 588 nm light. Spectra for the three anomaloscope primaries are shown in Fig. 1(a). The anomaloscope used for participant screening in the present study is described in greater detail in Boehm et al. (2014).

Experiments were run using MATLAB 2007a. Stimuli were presented on a Diamond Pro 2070SB monitor (Mitsubishi, Tokyo, Japan). The gamma functions of the monitor were linearized using a photometer (United Detector Technologies, Hawthorne, CA) and color calibration was done with a PR650 spectroradiometer (Photo Research, Inc., Chatsworth, CA). A Visual Stimulus Generator (VSG) 2/4 graphics card (Cambridge Research Systems, Rochester, UK) was used to generate experimental stimuli. Participants indicated their responses to stimuli with a Cambridge Research Systems CT3 Response Box.

4. Stimulus

Fig. 1b shows the spatial layout of the stimulus. The stimulus was a set of four sectors from an annulus with inner radius 0.85° and outer radius 2.1°, presented against an equal-energy grey background. The sectors and the gaps between them each comprised an eighth of the annular area, with the width of each sector spanning 1.27° of visual angle (the distance between the inner and outer radii of the annulus). There was a central black fixation dot.

Because perceptual isoluminance varies among individuals and especially for anomalous trichromats, we determined the relative intensities of the red, green and blue phosphors needed to achieve perceptual isoluminance for each participant using the minimum motion task (see Anstis & Cavanagh, 1983) available in Pyschtoolbox3 (PTB-3: Brainard, 1997; Pelli, 1997; Kleiner, Brainard, & Pelli, 2007).

As a color metric we used the MacLeod and Boynton (1979)

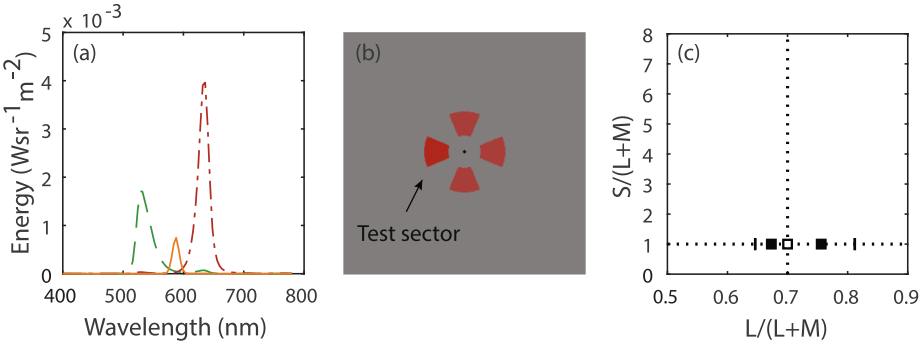

Fig. 1. Stimuli for the anomaloscope (a) and pedestal discrimination task (b, c). The left panel (a) shows the radiance spectra of the anomaloscope green (dashed), orange (solid), and red (dashed-dotted) primaries. The center panel (b) shows the spatial layout of the four-sector stimulus used in the 4-AFC discrimination task. The right panel (c) shows the coordinates of the pedestal stimuli in MacLeod-Boynton chromaticity space for green and red pedestals (filled squares), and the white pedestal (open square). Dotted lines are the cardinal axes of the MacLeod-Boynton chromaticity diagram. Line marks along the L/(L + M) axis denote the range of isoluminant test chomaticities within the display gamut after adjusting the stimulus luminance for each individual.

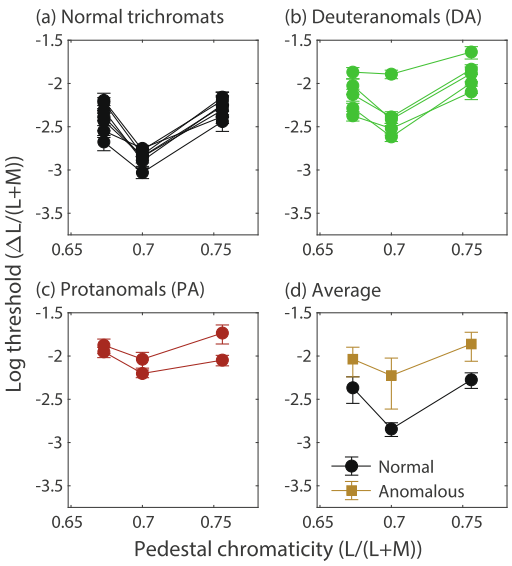

Fig. 2. Estimates of thresholds as a function of pedestal chromaticity. (a–c) show results for individual participants: (a) normal trichromats, (b) deuteranomals (DA), (c) protanomals (PA). Error bars are 95% bootstrap confidence intervals. Panel (d) shows the results averaged across normal (black, circle markers) and anomalous trichromats (orange square markers). Error bars are 95% confidence intervals of the mean estimate. For green and red pedestals (L/(L + M) = 0.6730, L/(L + M) = 0.7560), the x-coordinates show the fixed midpoint in chromaticity between the test and distractors, while the actual chromaticities of the test and distractor sectors presented on each trial were varied according to a staircase procedure (see *Procedure* for details). For white pedestals (L/(L + M) = 0.7) the distractors always equaled the pedestal chromaticity, with the test chromaticity either an increment or decrement along the L/(L + M) axis.

chromaticity diagram with the Stockman, MacLeod, and Johnson (1993) cone fundamentals, scaled so that the coordinates of equal-energy white were S/(L + M) = 1 and L/(L + M) = 0.7. Depending on the condition, the stimulus had one of three "pedestal" chromaticities, corresponding roughly to green (L/(L + M) = 0.6730), white (L/(L + M) = 0.7, identical to the background), and red (L/(L + M) = 0.7560). The pedestal chromaticities were selected to be 50% of the distance, in MacLeod-Boynton units, between equal-energy white and the gamut limit along the L/(L + M) cardinal axis (Fig. 1c).

We chose the luminance of the test stimuli so that the gamut limits along the L/(L + M) axis allowed for the maximal range of chromaticities achievable by the CRT monitor. To do this, we used each participant's luminance settings to find the "purple gamut limit," the most intense displayable stimulus for which S/(L + M) = 1 and the green phosphor was zero, and used this as the luminance of the test patches. The mean luminance of the test patches was approximately 22.65 cd/m^2 (SD = 1.1) for normal trichromats, 25.34 cd/m^2 (SD = 0.43) for deuteranomals, and 10.1 cd/m^2 (SD = 0.75) for protanomals. Thus, the luminance of the test stimuli was lower for protanomals than for the other two groups, but luminance is not expected to have a significant impact on the slopes of the function relating color discrimination to pedestal contrast (Yeh, Pokorny, & Smith, 1993), which was our primary measure of interest. The rationale for individual test luminances was that the range of isoluminant test chromaticities within the display gamut was the same for each participant (Fig. 1c). The equal-energy grey background (L/(L + M) = 0.7, S/(L + M) = 1) had luminance 80% of that of the test patches.

4.1. Procedure

On each trial, one sector was randomly chosen to be the "test" sector, and the other three were designated as the "distractor" sectors. In a four-alternative-forced-choice (4-AFC) task participants indicated which sector appeared to be of a different color than the other three by pressing the corresponding button on the response box. Stimuli were presented for up to 3 s and were removed immediately after a participant's response. There was a 2 s inter-trial interval, and participants were given auditory feedback indicating either a correct or incorrect response. To minimize adaptation, trials alternated between the pedestal conditions sequentially, where red, white, and green pedestals were tested in separate trials.

Two, interleaved (2-up-1-down) staircases were used for each pedestal condition in order to measure the difference in chromaticity (ΔL/(L + M)) required to discriminate between the test and distractor sectors correctly 82% of the time. In the white pedestal condition, the distractor sectors were metameric with equal-energy white (S/(L + M) = 1, L/(L + M) = 0.7) and the test sector was randomly either an increment or decrement in chromaticity along the L/(L + M) axis of the MacLeod and Boynton (1979) chromaticity diagram (Fig. 1c). For the red and green pedestal conditions, half of the ΔL/(L + M) determined by the staircase was added or subtracted from the chromaticities of the test and distractor stimuli so that the average of the two chromaticities was equal to the pedestal chromaticity on each trial (L/(L + M) = 0.7560 for red pedestals and 0.6730 for green pedestals). The test sector was always the most saturated. For example, in the red pedestal condition, the distractor sectors had L/(L + M) = 0.7560 - ΔL/(L + M)/2, and the test sector had L/(L + M) = 0.7560 + ΔL/(L + M)/2. For green pedestals, distractor sectors had L/(L + M) = 0.6430 + ΔL/(L + M)/2, and the test sector had L/(L + M) = 0.6430 - ΔL/(L + M)/2.

Each experiment session consisted of eight blocks of 121 trials each, with a 20 second break between each block. The staircases carried over between blocks, thus two staircases were completed per pedestal condition in each experiment session. Within each session, all six staircases were interleaved in repetitions of groups of 6 trials in a fixed order: Green pedestal (staircase 1), white pedestal (staircase 1), red pedestal (staircase 1), green pedestal (staircase 2), white pedestal (staircase 2), red pedestal (staircase 2). There were 160 trials per staircase. The first trial in each block was a randomly selected "sham trial" which was not included in the data analyses but intended to mitigate the risk of participants missing the first trial in a block. Each participant completed the experiment twice, culminating in four staircases for each pedestal condition.

5. Results

Thresholds for chromatic discrimination were measured for each of the three pedestal conditions. Data from the four staircases for each participant were combined and fit with a cumulative Gaussian psychometric function, where the 82% point was defined as threshold. A bootstrap analysis was performed where, for each participant, we resampled at the trial level from the combined data (from all staircases) with replacement and fit cumulative Gaussians to each resampling of the data. Thresholds were then recalculated over 10,000 iterations. Fig. 2 shows the threshold estimates for each of the individual participants (a–c), and the means for normal and anomalous trichromats (d). Error bars represent 95% confidence intervals from the bootstrap analysis for individual participant data, and the 95% confidence interval for the mean across participants using the Students' t-distribution.

The results for color normal observers show the familiar V profile when the log of the discrimination threshold is plotted against pedestal chromaticity. From the minimum of the V where pedestal chromaticity is the same as the background (zero chromatic contrast), the log base 10 of the discrimination threshold went up by 0.477 for the green pedestal and by 0.569 for the red pedestal, meaning that the chromaticity

difference required for reliable discrimination increased by factors of 3.00 and 3.70 respectively. We attribute this increase to post-receptoral response compression in the normal trichromatic visual system.

For participants with normal color vision there were slight differences in the overall thresholds, but the slopes of the threshold vs. pedestal saturation functions (the two sides of the V) were largely consistent. On average, thresholds for deuteranomals and protanomals with the achromatic pedestal were 3.66 and 5.40 times greater than for normal, respectively, though with considerable individual variation.

More significantly, the anomalous discrimination thresholds also show a V shaped profile indicating impaired discrimination performance (higher thresholds) in the presence of the saturated pedestals. Notably, the superiority of anomalous participants, that was entertained as a theoretical possibility in the Introduction, did not materialize: the anomalous participants remained on average less sensitive than normal trichromats with saturated pedestals, as shown by their higher thresholds. For the white pedestals, all anomalous participants had higher thresholds than normal trichromats. However, we note that two deuteranomals had thresholds for green pedestals that were within the normal range. The key test of the neural compensation hypothesis, however, lies in the slopes of the V, that express the extent of the chromatic discrimination deficit associated with the chromatic pedestals.

Fig. 3 compares the slopes of the V contours for deuteranomals and protanomals with those of normal trichromats, and also to what would be expected under Full and Zero Compensation models. The dashed lines show the mean steepness of the V slope from the normal trichromats' thresholds, shifted rigidly upwards to bring them into coincidence with each anomalous participant's threshold at zero pedestal chromatic contrast. The dotted lines show the thresholds predicted from the Zero Compensation model. These were calculated by dividing the slope of the mean V contour for normal trichromats by a factor, *k*, expressing the chromatic sensitivity deficit of each individual anomalous observer relative to the mean of the normal trichromats' thresholds (i.e. an outward scaling of the normal V from the grey point). The value of *k* was simply the ratio of the individual anomalous participant's discrimination threshold to the mean of the normal trichromats, obtained with the achromatic pedestal in each case. The rationale for this construction is provided in 'Models' below.

The V slopes for anomalous observers fail to conform exactly either to the slope of normal trichromatic observers or to the Zero Compensation model prediction, but generally fall between these limits. One-tailed, two-sample *t*-test showed that the anomalous observer's V slopes (average of the two slopes corresponding to each arm of the V function) are reliably shallower than those of normal trichromats ($t(12) = -3.1$, $p = .0045$) and also steeper than the Zero Compensation model prediction ($t(12) = 2.02$, $p = .033$). Thus, the results do fulfill our prediction that anomalous observers perform better with a pedestal than without (in the sense that their log threshold is closer to that of normal trichromats when measured with red and green pedestals compared to white), but the improvement that they show is not as great as expected on the hypothesis of zero compensation.

However, with our small sample size and large individual differences, it is likely that the results of the *t*-test showing significantly shallower slopes is driven by the most extreme participants (e.g., DA5), while some participants conform to the slopes obtained from normal trichromats (e.g., DA3). In some cases, the threshold and error estimates appear to conform equally well to both the Full and Zero Compensation models (e.g. PA2). To compare slopes between individual participants, we assessed the 95% confidence intervals around the slope estimates obtained from our bootstrap analysis. These are shown in the bottom right panel of Fig. 3, with participants separated by group along the x-axis. Slopes for deuteranomals and protanomals follow the same order as the individual results presented in the other figure panels. Comparing the absolute values of the slopes obtained from anomalous trichromats and their confidence intervals revealed that the slopes for the two arms of the V function did not differ significantly (in the sense that their confidence intervals overlapped), except for PA1 who had a significantly steeper slope in the -L/(L + M) (green) direction than for the +L/(L + M) (red) direction.

The participants with the shallowest slopes (closest to the zero compensation prediction) also had the largest matching ranges over their five anomaloscope settings. Of the deuteranomals, participants DA2 and DA5 had matching ranges that were approximately 2 and 4 times greater, respectively, than the mean matching ranges of the other three deuteranomalous participants. Participant PA1′s matching range

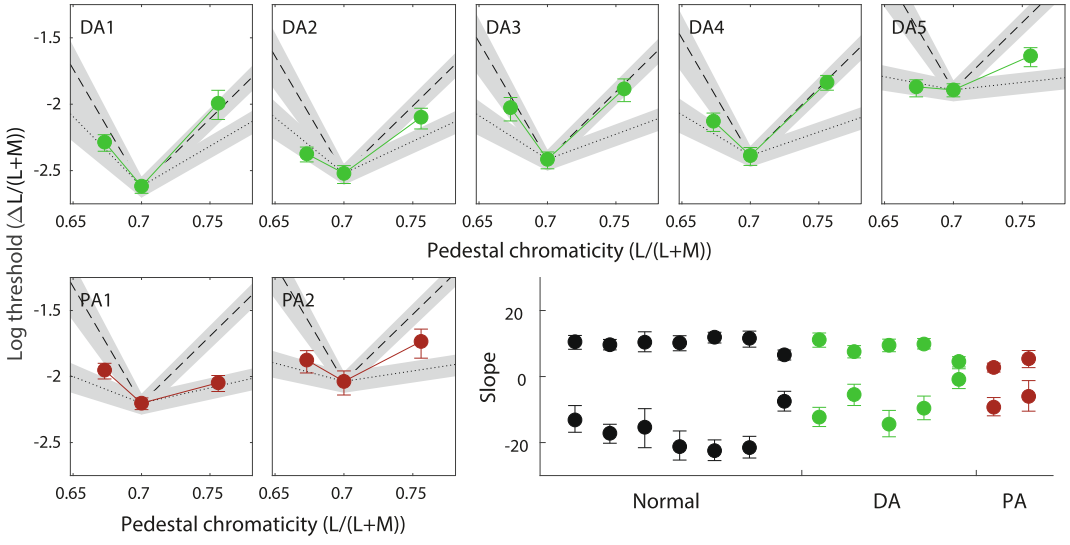

Fig. 3. Comparison of results for anomalous trichromats with normal trichromats and with predictions for the Zero Compensation model. Threshold estimates and V contours are shown for individual deuteranomals (green) and protanomals (red), along with the translated V contours for normal trichromats (dashed gray lines) and predictions under the Zero Compensation model, (dotted gray lines), respectively. Shaded gray regions represent the 95% confidence intervals for the mean normal trichromat threshold estimates and the threshold estimates under the Zero Compensation model where the slopes are reduced by a factor *k*. The bottom right panel shows the slope estimates for each participant, separated by group along the x-axis (with ordering the same as in the preceding panels): normal (black), deuteranomals (DA, green) and protanomals (PA, red). Error bars are 95% confidence intervals of the slopes estimated in a bootstrap analysis. Negative slopes correspond to the green pedestal condition (-L/(L + M)) and positive slopes to the red pedestal condition.

was approximately 3 times greater than participant PA2's. A one-tailed Spearman correlation confirmed a significant negative association between participants' matching ranges, defined here as the largest Euclidean distance between the coordinates of the matches in the MacLeod-Boynton chromaticity diagram, and the average of each participant's slopes shown in Fig. 3 ($rs(5) = -0.75$, $p = .033$). However, it should be noted that we did not directly measure matching range and the full matching ranges for each participant are likely not captured by their five anomaloscope settings. This, along with our small sample size, preclude us from making any general conclusions about the relationship between anomaloscope settings and post-receptoral compensation.

6. Models

In this section we present the predictions of different theoretical possibilities for how post-receptoral compensation, or its absence, would affect chromatic discrimination at the achromatic point and on chromatic pedestals. First, we consider expectations under a Zero Compensation model where signals at the receptor level are reduced by the greater spectral overlap of the anomalous long and medium wavelength sensitive cones, but post-receptoral processing occurs as it does in normal trichromats. Second, we model thresholds under the assumption of post-receptoral compensation, and present predictions for different degrees of postreceptoral compensation. Lastly, we consider the likely effects of neural noise on thresholds given different assumptions about the predominant source of neural noise, and specifically whether the predominant source of neural noise occurs before or after post-receptoral compensation.

7. Predictions assuming zero compensation

To model the variation of color discrimination threshold with pedestal chromaticity in anomalous observers (and abbreviating L/(L + M) as r), we begin by noting the empirically supported rough linearity between log threshold and $|r_{ped}\text{-}r_w|$ (where r_{ped} refers the pedestal chromaticity and r_w to the white background), defining what we have called the V profile in normal trichromatic observers (Miyahara et al., 1993; MacLeod, 2003). Specifically, the decimal log threshold measured with r_{ped} exceeds the value for r_w by $(|r_{ped}\text{-}r_w|)/r_{10}$, where the constant r_{10} is the reciprocal of the slope of the V shaped profile in plots such as Fig. 3. It represents the absolute deviation of pedestal chromaticity from white, $|r_{ped}\text{-}r_w|$, that would raise threshold tenfold.

The V profile relating discrimination threshold to pedestal chromaticity is expected for a system where post-receptoral neurons have compressively nonlinear responses to the chromatic contrast supplied by the pedestal, and where discrimination is limited by noise introduced at the nonlinearly compressed output—for example by fluctuations of impulse counts in the firing of retinal ganglion cells, if the nonlinear encoding of chromatic contrast is already present at the level of retinal ganglion cells (see for instance Pugh & Mollon, 1979; von der Twer & MacLeod, 2001; MacLeod & von der Twer, 2003).

In the model, the cone photoreceptor signals provide the input to these second stage neurons, directly or indirectly. The quantity $|r_{ped}\text{-}r_w|$ is a measure of the chromatic contrast associated with a pedestal, defined in terms of the photoreceptor excitations of normal trichromats. Note that the selection of $|r_{ped}\text{-}r_w|$ as the measure of contrast is not critical for an approximate analysis, since other candidate measures of chromatic contrast are approximately proportional to $|r_{ped}\text{-}r_w|$. For an anomalous observer, the same function of the cone outputs defines an analogous 'effective' chromatic contrast. But because cone quantum catch varies smoothly and approximately linearly with small variations in λ_{max}, the imbalance in cone quantum catches elicited by a colored pedestal is scaled approximately in proportion to the separation between the pigment absorption spectra. If we posit that white is represented as in normal trichromacy (at the center of an opponent neuron's operating range), chromatic contrasts from white are effectively scaled by 1/k, the ratio of anomalous pigment separation to that of normal trichromats.

Following MacLeod and von der Twer (2003), we adopt an idealized model in which chromatic discrimination requires a reliable difference in some relevant chromaticity-dependent neural output signal, N. On that assumption, discrimination threshold varies inversely with the slope of the neural output N with respect to stimulus chromaticity. The linearly increasing relation between log threshold and pedestal chromatic contrast means that threshold increases exponentially with pedestal contrast. If we assume for simplicity that σ_N, the random variability introduced by random noise into the neural output N is independent of the input, this exponential increase in threshold must originate from an inverse change in slope: The slope must be exponentially decreasing, varying as $10^{-(|rped\text{-}rw|)/r10)}$ or $e^{-(2.3*(|rped\text{-}rw|)/r10)}$, where r_{10} is the value of $|r_{ped}\text{-}r_w|$ that produces a 10 fold (1 $\log_{10}$ unit) elevation of threshold. The parameter r_{10} scales contrast for all observers and was fixed at a value determined by the mean steepness of the V slope (averaged over red and green pedestals) for our sample of normal trichromats. To simplify notation we write C for the measure of pedestal contrast forming the base *e* exponent:

$$C = 2.3*\left(|r_{ped} - r_w|\right)/r_{10} \quad (1)$$

so that with a suitable choice of unit for N:

$$dN/dr = e^{-C} \quad (2a)$$

and

$$dr/dN = e^{C} \quad (2b)$$

The observer uses the noise-contaminated output signal $N \pm \sigma_N$ to estimate the input (here, the stimulus chromaticity r). The discrimination threshold Δr is defined by the standard deviation (over multiple trials) of the observer's estimate of r, which is simply the standard deviation of the output σ_N divided by the slope of the output with respect to pedestal contrast r, dN/dr for the normal trichromat:

$$\Delta r = \sigma_N * e^{C} \quad (3a)$$

For the anomalous observer with sensitivity 1/k, modifying Eq. (2a), $dN/dr = (1/k)*e^{-C/k}$, and

$$\Delta r = k\sigma_N * e^{C/k} \quad (3b)$$

The normal trichromat's threshold with a white pedestal (where C = 0) is just σ_N, and this establishes the value of σ_N. For our data, $\sigma_N = 10^{-2.84}$. With this substitution of σ_N into Eq. (3a) we obtain the threshold as a function of pedestal contrast C, as $10^{-2.84}*e^{C}$ for the normal observer and by substituting into Eq. (3b), $k*10^{-2.84*}e^{C/k}$ for the anomalous observer.

Ideally, the factor k would be estimated from knowledge of the pigment absorption spectra, but in Fig. 3 we estimated it as the ratio of the anomalous threshold on white to the normal threshold. Fig. 4 elaborates on Fig. 3 by showing the predicted thresholds under the Zero Compensation model for a range of plausible values of k, resulting from different degrees of spectral overlap of the anomalous medium and long wavelength-sensitive photopigments. The average anomalous threshold for the white pedestal is consistent with a k of 4.12, equating to about a 7 nm spectral separation for the anomalous pigments, a value roughly consistent with a published prediction based on average anomaloscope matching data (DeMarco, Pokorny, & Smith, 1992). This suggests that anomalous observers do not benefit much from compensation for discrimination of targets on a white pedestal.

The reduced V slopes that are both theoretically expected and experimentally observed for anomalous observers (Fig. 2) show that the discrimination deficit associated with anomaly is generally considerably less than is typically measured experimentally using a bipartite field (because color discrimination in practice often involves comparison of separate colors, each clearly distinct from the immediate surround – the suprathreshold pedestal case – whereas bipartite field discrimination

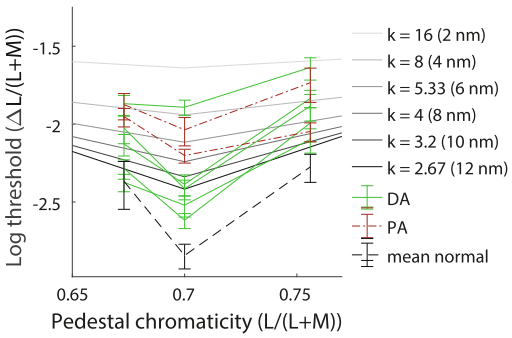

Fig. 4. Predictions of the zero-compensation model for different spectral separations. Gray solid lines show modeled thresholds as a function of pedestal chromaticity, following Eq. (3b). Each line corresponds to a different estimate of k, the ratio of the normal to anomalous spectral separations. A 32 nm separation was assumed for normal trichromats, and k ratios were calculated for spectral separations of 2 to 12 nm (in 2 nm steps). Individual participant data are shown for comparison, with green solid lines for deuteranomals and red dashed-dotted lines for protanomals.

corresponds to the zero contrast pedestal case, where the anomalous threshold is most elevated above the normal trichromats'). The present analysis further suggests that anomalous discrimination performance for stimuli that have high chromatic saturation relative to their background could even be superior to the performance of normal trichromats. In our present model this condition arises when the anomalous and normal threshold-versus-pedestal chromaticity curves cross. The cross point occurs where Eq. (3a) = Eq. (3b) (substituting for C using Eq. (1)): $|r_{ped} - r_w|/r_{10} = \log(k)*k/(k-1)$, thus *anomalous superiority* is theoretically expected when the threshold elevation by the chromatic pedestal exceeds $\log(k)*k/(k-1)$ for normal trichromats, or about 0.8 $\log_{10}$ units for k = 4 (corresponding to an 8 nm pigment separation). This condition was never attained in our data, however. Large enough threshold elevations were not reached for normal trichromats at the pedestal contrasts used, and besides, the anomalous V slopes were not as shallow as the model predicts (Fig. 4).

8. Predictions assuming post-receptoral compensation

Can post-receptoral compensation explain the finding that the anomalous V slopes were not as shallow as predicted? A compensation that takes the form of a uniform upscaling (i.e., amplification) of contrast in the post-receptoral neural representation simply undoes (partially or completely) the effect of the pigment swap, effectively changing the value of k in the model without improving the predictions.

In formal terms, for the anomalous observer with sensitivity 1/k, and partial compensation effectively upscaling contrast by j, the upscaled input to the compressive nonlinearity is an effective contrast of j*(C/k), and

$$dN/dr = j/ke^{-j*C/k} \quad (4)$$

Thus, by analogy with Eq. (3b)

$$\Delta r = (k/j)\sigma_N e^{j*C/k} \quad (5)$$

For full compensation, j = k making the slope of output with respect to input, and hence the threshold, the same as for the normal trichromat. More generally, as the equation shows, the effect of compensation that is uniform across all pedestal contrasts is simply to mimic a reduced anomalous sensitivity deficit, making anomalous performance less different from normal than would be inferred from the pigment spectra on the assumption of zero compensation. This will generally reduce the discrimination threshold. A suitable choice of j allows the anomalous V slopes to be made steep enough, but only by making the predicted anomalous thresholds approach the thresholds of normal trichromats along the entire slope of the V (Fig. 5, upper row), in conflict with the observed elevation of the anomalous thresholds on white. So, this model fails to capture the experimental results.

Further theoretical possibilities include the assumption of different forms for the contrast-response function. With a linear function, the theoretical framework cannot predict the steeply sloping V profiles. With a logarithmic transform, a uniform upscaling of contrast has no effect at all, either on predicted thresholds or on the required anomalous deficit k. This follows from the relation

$$d(log(C))/dC = d(log(C/k))/dC \quad (6)$$

and further highlights the unexpectedly subtle connection between compensation and discrimination. As noted, with pedestal contrasts that sufficiently elevate thresholds for normal trichromats, the model of Eq. (3b) does provide for anomalous superiority to normal in discrimination on the assumption of zero compensation at sufficiently high contrast. In that case, post-receptoral compensation could actually be deleterious for anomalous discrimination, by overloading the chromatic contrast signals. But that situation was not realized in our experiments. Under our conditions the effect of chromatic pedestals was only to reduce the anomalous color discrimination deficit (an effect seen in the reduced V slopes for anomalous participants), not eliminate or reverse it. As we have noted (Fig. 3), our anomalous V slopes are not reduced as much as theoretically expected on the hypothesis of zero compensation. Within our idealized model, however, post-receptoral compensation cannot explain this.

9. Effect of photoreceptor noise

In anomalous trichromats, the location of the predominant source of neural noise—and particularly whether it occurs before or after putative post-receptoral compensation—affects the predicted shape of the function describing discrimination threshold as a function of pedestal chromatic contrast. If the neural noise that limits discrimination performance is receptoral or otherwise occurs *before* the post-receptoral transformation of the sensory signal then the noise will be transformed along with the signal. Since it is the signal to noise ratio that determines threshold, in this scheme thresholds would not be altered, though suprathreshold perceptual differences would be altered according to the transformation. On the other hand, if the performance-limiting source of neural noise occurs *after* post-receptoral compensation (as we have assumed for simplicity so far), this noise would not be amplified along with the signal, and therefore chromatic discrimination thresholds would be lowered (relatively normalized) as a result of post-receptoral compensation. The precise predictions for the effect of pre- and post-compensation neural noise on the shape of the function describing chromatic detection threshold with pedestal saturation depend on the proportions of early and late noise and on the degree of post-receptoral compensation. We outline predictions for the different scenarios below.

Neural noise that occurs after the compressively nonlinear representation of saturation, which we call *output noise* is a crucial ingredient of the model we have described, because it interacts with the pedestal contrast to generate the predicted V profiles. But discrimination threshold also depends upon the level of *input noise* occurring before the compressive nonlinearity – such as noise introduced by activity in the photoreceptors. Input noise should be relatively independent of pedestal chromatic contrast in the range of interest because the receptor signals that provide inputs are only slightly perturbed by changes in contrast that are within the limited range used in our experiment. We incorporated input noise into our idealized (Zero Compensation) model by adding a component σ_{in}^2 to the variance in the participant's estimate of stimulus chromaticity r, statistically independent of the output noise and

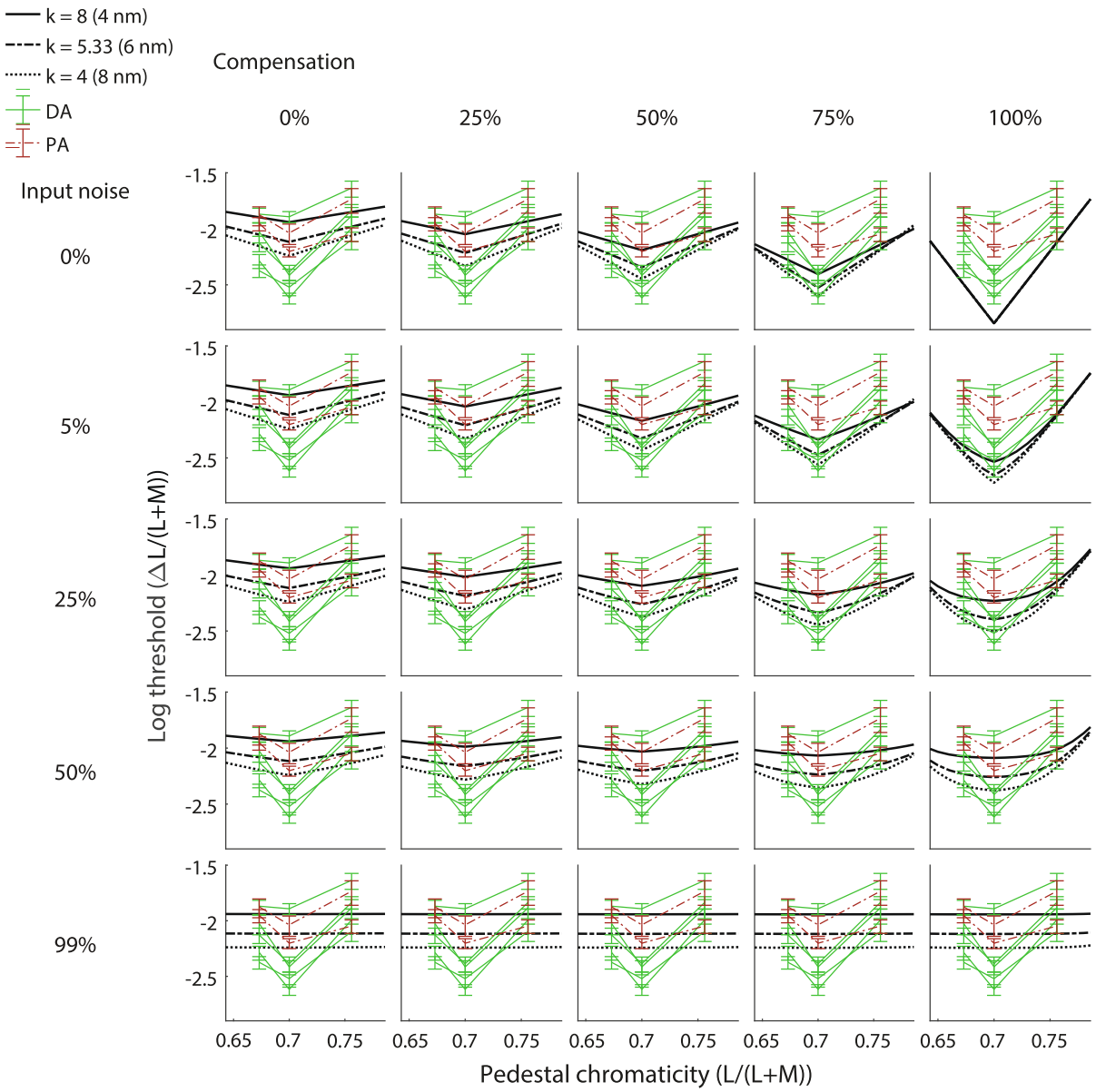

Fig. 5. Model predictions for various amounts of input noise and post-receptoral compensation. Each row corresponds to a different percentage of input noise, which represents the fraction of total noise in the normal trichromats' zero pedestal threshold that occurs before the compressive nonlinearity. Each column in the figure corresponds to a different percentage of post-receptoral compensation. Predictions for different k values are shown, corresponding to 4 nm (k = 8), 6 nm (k = 5.33) and 8 nm (k = 4) spectral separations. Individual data are shown for comparison to the model (green solid lines for DAs and red dashed-dotted lines for PAs). (For interpretation of the references to color in this figure legend, the reader is referred to the web version of this article.)

independent of chromatic contrast. Thus instead of Eq. (3b) we have

$$\Delta r = \left(\left(k\sigma_N e^{(C/k)} \right)^2 + \sigma_{in}^2 \right)^{1/2} \quad (7)$$

For our initial model with only output noise (Fig. 5, top row), compensation by uniform upscaling of contrast could not fit our data. But with the addition of significant input noise, considered as a percentage of total (input + output) noise in the normal trichromats' estimate of r, the effects of compensation by uniform upscaling of contrast are more complex. Fig. 5 shows predictions of the model when input noise is considered. In the figure, each row of panels corresponds to a different percentage of input noise, and each column a different level of compensation. In the model, input noise is scaled by compensation along with the signal, so is scaled by factor k for the anomalous observer. For full compensation, output noise for an anomalous trichromat is the same as for a normal trichromat, since contrast is compensated before the compressive nonlinearity. In the Zero and Partial Compensation models, output noise is scaled by either k or k/j, respectively, to reflect the reduced effective contrast at the input to the compressive nonlinearity.

According to Eq. (7), the effect of output noise is greatest with pedestals of high chromatic contrast C, and least with C = 0, where the effects of input noise are therefore clearest. For this reason, when input noise (which we assume occurs before post-receptoral compensation) is substantial, a uniform upscaling of effective contrast as would occur with post-receptoral compensation brings relatively little benefit in the zero pedestal contrast condition—much as if the compensation were not effective there.

In this way, input noise can create the failure of reciprocity between threshold and V slope implicit in the deviation of the data of Fig. 3 from the model predictions when only output noise in considered (Fig. 5, first row). This raises the possibility that post-receptoral compensation in conjunction with photoreceptor noise could provide a good account of

those data. Fig. 5 shows, however, that input noise could not fully remedy the predictions of the Full Compensation model (Fig. 5, column 5). The anomalous V slopes could be reasonably well predicted by incorporating input noise slightly less than the output noise (e.g., rows 2 and 3). The fit remained poor, however, because the expected threshold elevations for the anomalous observers in those cases were on average less than observed, for all pedestals. Further increase in input noise could predict the average anomalous sensitivity loss, but at the expense of making the V slope much too shallow.

10. Discussion

We measured chromatic discrimination thresholds for increments of saturation on pedestals at different points along the L/(L + M) axis of the MacLeod-Boynton chromaticity diagram in anomalous trichromats and compared them to those of normal trichromats. The sensitivity deficit shown by the anomalous observers, expressed as an elevation of log threshold relative to the performance of normal trichromats, was less pronounced in the presence of red or green pedestals, but even under those conditions the anomalous observers did not attain or exceed performance of normal trichromats in discrimination for the pedestal saturations tested.

For all observers, color discrimination thresholds were higher for red and green pedestals than for white ones, but threshold elevations were less for anomalous trichromats than for normal trichromats. As we suggested in the introduction, this is qualitatively expected if the anomalous visual system is post-receptorally normal, since the reduced chromatic difference signals that originate from the anomalous photoreceptors should be less effective in driving post-receptoral color-coding neurons into the compressively nonlinear range of their contrast-response functions, thereby allowing these neurons to better preserve their differential sensitivity.

Zero compensation? In a simple idealization of the Zero Compensation model, outlined in the subsection '*Predictions assuming zero compensation*', the anomalous observer behaves like an observer with normal trichromacy stimulated by pedestals of reduced chromatic contrast. The reduction is by a factor equal to the anomalous observer's chromatic sensitivity deficit. The slopes of the theoretical V-shaped profile relating log color discrimination threshold to pedestal chromaticity (dotted curve, Fig. 3) are correspondingly reduced from normal by that factor. The premise for this prediction is that the post-receptoral organization of the visual system of anomalous observers is completely normal, without any neural compensation to remedy the deficit associated with the pigment swap. On this Zero Compensation model, the anomalous trichromat's pigment swap reduces the effective chromatic contrast signaled by long-wave and middle-wave sensitive cones by the same factor for pedestal and for test stimulus alike. A pedestal with high chromatic contrast that saturates a color contrast encoding neuron in the normal trichromat may therefore fail to saturate it in the anomalous observer.

Post-receptoral compensation? Although the V slopes of most of the anomalous observers in Fig. 2 are indeed shallower than the slopes of normal trichromats, as predicted, the results are not fully consistent with the Zero Compensation model. The slopes generally fall between the model prediction and the steeper slopes characteristic of normal trichromats. This could suggest that the model's predictions might be improved by adding a feature that makes the anomalous neural representation of contrast more similar to that of the normal trichromat-specifically a neural compensation where post-receptoral signals are amplified to span the full normal range.

Uniform compensation? The simplest form of compensation would be a post-receptoral amplification that increases all effective contrasts by the factor that was lost owing to the spectral proximity of the anomalous pigments, thereby reinstating-or approximating-the relationship between the neural output and stimulus chromaticity in normal trichromacy. The effective contrast for the anomalous cones C_a having been reduced at the photoreceptor level from the value C for normal trichromats to C/k (in the notation of the 'Models' section), could hypothetically be restored to the normal value in the post-receptoral transformation that forms the chromatic contrast signals. But in that scenario, and with the assumption that discrimination is entirely limited by output noise (occurring after the compressive nonlinearity in the representation of saturation and after post-receptoral compensation), the fully compensated anomalous observer would show performance identical to the performance of normal trichromats under all conditions, contrary to the reduced sensitivity of anomalous trichromats that is ordinarily seen in discrimination tasks (such as matching in a bipartite anomaloscope field).

We also discussed a generalization of this scheme, with partial rather than complete compensation (amplification by a factor j which is less than k). This may appear promising because it predicts anomalous V slopes steeper than expected with no compensation, but shallower than the slopes of normal trichromats. But as Fig. 5 shows, it fails to fit our data, because along with the steeper V slope it necessarily predicts too low an anomalous threshold at the bottom of the V. For any uniform rescaling of chromatic contrast, the V slope predicted for each anomalous observer is inversely related to the anomalous sensitivity deficit expressed in the ratio of anomalous to normal thresholds with an unsaturated pedestal. In Fig. 3, the zero compensation predictions (dotted curves) embody that reciprocity—being determined by the observed thresholds on a white pedestal—but the steeper-than-predicted observed anomalous V slopes of Fig. 3 violate it. So the Partial and Full Compensation models, shown in the top row of panels in Fig. 5, cannot correct the shortcomings of the Zero Compensation model. In fact, the effect of compensation by uniform upscaling is merely to change the value of the parameter k that defines the anomalous sensitivity deficit, effectively reducing it and generally lowering, rather than increasing the predicted threshold. The failure of complete or partial post-receptoral compensation to fit our data leads us to conclude that the theoretical scheme so far is incomplete, so we considered promising elaborations of it by considering the role of early (input) neural noise.

Though the strong influence of pedestal contrast on threshold implies an important role for late *output* noise originating in contrast-driven neurons, it is natural to assume that early *input* noise occurring before the compressive nonlinearity (including photoreceptor noise) is significant as well. Without input noise, compensation by uniform upscaling of contrast does not affect the behavior of the model, but merely mimics a sensitivity change, as we have noted. With substantial input noise, this is no longer true. In a model incorporating input noise (see 'Models' *3. Effect of photoreceptor noise*), the V profiles are theoretically rounded into U profiles, and the V slopes are decreased for all observers (Fig. 5). The V slopes theoretically associated with a given threshold elevation are generally reduced, whereas a fit to the data would require increased slopes. However, once again, the steeper than predicted anomalous V slopes of Fig. 3 could only be modeled by generating far too low a threshold for the white pedestal, at the bottom of the anomalous V. Thus, post-receptoral compensation of the forms we have considered does not seem to be helpful in completely accounting for our experimental findings, even when input noise is incorporated into our simple model.

Suprathreshold compensation only? Another promising, but ultimately inadequate way to improve the model is to assume that compensation is not uniformly effective for all contrasts, but applies only in a suprathreshold contrast range. This would allow the full anomalous sensitivity deficit associated with the pigment swap to appear under low contrast conditions, but could at the same time generate larger sensitivity losses on chromatic pedestals than the uncompensated model predictions. There is a clear functional rationale for this proposal. Neural compensation can hardly work well near threshold, where there may be no signal to amplify, or the signal may already be so contaminated by random noise that it is best ignored. So, might compensation be confined to stimuli with high enough contrast to generate clear signals even in the

anomalous observers? The posited process is analogous to the 'contrast constancy' invoked to explain nearly veridical matching of contrast between different spatial frequencies that have very different contrast thresholds (Georgeson & Sullivan, 1975), in that thresholds for anomalous trichromats and normal trichromats could be very different but they may have (between-observer) "contrast constant" perception of suprathreshold chromatic contrasts caused by post-receptoral compensation. However, the effect of compensation that is suprathreshold only is to pull the predicted anomalous thresholds on the colored pedestals downwards toward the thresholds of normal trichromats. This is the wrong direction to account for the upward deviations from the dotted curves of Fig. 3.

Of course, a more elaborate model might introduce features designed to help fit the data. For example, suprathreshold compensation might itself be a source of randomness; fluctuations in gain at high amplification could then lead to higher anomalous thresholds on the chromatic pedestals. Similarly, we could consider noise that occurs later than the stage at which there is a compressively nonlinear representation of saturation but earlier than the stage at which post-receptoral compensation occurs (e.g. noise at the level of retinal ganglion cells but post-receptoral compensation in cortical neurons).

To conclude: We have seen that the sensitivity deficit shown by anomalous trichromats in color discrimination at low chromatic contrast is reduced when discriminating between stimuli of high chromatic contrast. Because such comparisons are a common challenge in daily life, the findings imply that anomalous trichromats are not as disadvantaged as standard experimental measures suggest. Such a benefit is expected if anomalous observers escape the second-site sensitivity losses associated with contrast compression in chromatic signals that is observed in normal trichromats. While the results we present here refute the hypothesis of post-receptoral normality (zero compensation), and suggest some reorganization of the anomalous trichromatic system in response to developmentally challenged inputs, they do not support the specific forms of the compensation hypothesis that we have considered as simple alternatives.

CRediT authorship contribution statement

Alexandra E. Boehm: Software, Formal analysis, Investigation, Writing - original draft, Visualization, Project administration. **Jenny Bosten:** Methodology, Software, Formal analysis, Writing - original draft, Visualization. **Donald I.A. MacLeod:** Conceptualization, Methodology, Software, Formal analysis, Resources, Writing - review & editing, Supervision, Funding acquisition.

Acknowledgements

Funding: This work was supported by the National Institutes of Health [grant numbers EY01711, T32EY7043-38]; the American Academy of Optometry Foundation Michael G. Harris Ezell Fellowship; and the Minnie Flaura Turner Memorial Fund for Impaired Vision Research.

References

Anstis, S. M., & Cavanagh, P. (1983). A minimum motion technique for judging equiluminance. In J. Mollon, & R. T. Sharpe (Eds.), *Colour vision: Physiology and psychophysics* (pp. 155–166). London: Academic.

Barbur, J. L., Rodriguez-Carmona, M., Harlow, J. A., Mancuso, K., Neitz, J., & Neitz, M. (2008). A study of unusual Rayleigh matches in deutan deficiency. *Visual Neuroscience, 25*(3), 507–516.

Blessing, E. M., Solomon, S. G., Hasheimi-Nedhad, M., Morris, B. J., & Martin, P. R. (2004). Chromatic and spatial properties of parvocellular cells in the lateral geniculate nucleus of the marmoset (Callithrix jacchus). *Journal of Physiology, 557*, 229–245.

Boehm, A. E., MacLeod, D. I. A., & Bosten, J. M. (2014). Compensation for red-green contrast loss in anomalous trichromats. *Journal of Vision, 14*(13), 19.

Bosten, J. M., Robinson, J. D., Jordan, G., & Mollon, J. D. (2005). Multidimensional scaling reveals a color dimension unique to 'color-deficient' observers. *Current Biology, 15*(23), R950–R952.

Brainard, D. H. (1997). The psychophysics toolbox. *Spatial Vision, 10*(4), 433–436.

Bushnell, B. N., Harding, P. J., Kosai, Y., Bair, W., & Pasupathy, A. (2011). Equiluminance cells in visual cortical area V4. *Journal of Neuroscience, 31*(35), 12398–12412.

Chen, C.-C., Foley, J. M., & Brainard, D. H. (2000). Detection of chromoluminance patterns on chromoluminance pedestals I: Threshold measurements. *Vision Research, 40*(7), 773–788.

DeMarco, P., Pokorny, J., & Smith, V. C. (1992). Full-spectrum cone sensitivity functions for X-chromosome-linked anomalous trichromats. *Journal of the Optical Society of America A, 9*(9), 1465–1476.

Di Russo, F., Spinelli, D., & Morrone, M. C. (2001). Automatic gain control contrast mechanisms are modulated by attention in humans: Evidence from visual evoked potentials. *Vision Research, 41*(19), 2435–2447.

Georgeson, M. A., & Sullivan, G. D. (1975). Contrast constancy: Deblurring in human vision by spatial frequency channels. *The Journal of Physiology, 252*(3), 627–656.

Gomes, B. D., Souza, G. S., Rodrigues, A. R., Saito, C. A., Silveira, L. C. L., & Da Silva Filho, M. (2006). Normal and dichromatic color discrimination measured with transient visual evoked potential. *Visual Neuroscience, 23*(3-4), 617–627.

Kawamoto, K.-I., Inamura, T., Yaguchi, H., & Shioiri, S. (2003). Color discrimination characteristics depending on he background color in the (L, M) plane of a cone space. *Optical Review, 10*, 391–397.

Kaneko, S., Kuriki, I., & Andersen, S. K. (2020). Steady-state visual evoked potentials elicited from early visual cortex reflect both perceptual color space and cone-opponent mechanisms. *Cerebral Cortex Communications, 1*(1), 1–14.

Kleiner, M., Brainard, D. H., & Pelli, D. G. (2007). What's new in Psychtoolbox-3? *Perception, 36* (ECVP 2007 Abstract Supplement).

Knoblauch, K., Marsh-Armstrong, B., & Werner, J. S. (2020). Suprathreshold contrast response in normal and anomalous trichromats. *Journal of the Optical Society of America A, 37*(4), A133–A144.

Krauskopf, J., & Karl, G. (1992). Color discrimination and adaptation. *Vision Research, 32*(11), 2165–2175.

Lasley, D. J., & Cohn, T. E. (1981). Why luminance discrimination may be better than detection. *Vision Research, 21*(2), 273–278.

Lee, B. B., Pokorny, J., Martin, P. R., Valbergt, A., & Smith, V. C. (1990). Luminance and chromatic modulation sensitivity of macaque ganglion cells and human observers. *Journal of the Optical Society of America A, 7*(12), 2223. https://doi.org/10.1364/JOSAA.7.002223.

Lutze, M., Pokorny, J., & Smith, V. C. (2006). Achromatic parvocellular contrast gain in normal and color defective observers: Implications for the evolution of color vision. *Visual neuroscience, 23*(3-4), 611–616.

MacLeod, D. I. A., & Boynton, R. M. (1979). Chromaticity diagram showing cone excitation by stimuli of equal luminance. *Journal of the Optical Society of America, 69*(8), 1183. https://doi.org/10.1364/JOSA.69.001183.

MacLeod, D. I. A. (2003). Colour discrimination, colour constancy, and natural scene statistics (the Verriest lecture). In J. D. Mollon, J. Pokorny, & K. Knoblauch (Eds.), *Normal and defective colour vision* (pp. 189–218). London: Oxford University Press.

MacLeod, D. I., & von der Twer, T. (2003). The pleistochrome: Optimal opponent codes for natural colours. In D. Heyer, & R. Mausfeld (Eds.), *Colour perception: From light to object* (pp. 155–184). London: Oxford University Press.

Merbs, S., & Nathans, J. (1992). Absorption spectra of the hybrid pigments responsible for anomalous color vision. *Science, 258*(5081), 464–466.

Miyahara, E., Smith, V. C., & Pokorny, J. (1993). How surrounds affect chromaticity discrimination. *Journal of the Optical Society of America A, 10*(4), 545. https://doi.org/10.1364/JOSAA.10.000545.

Pelli, D. G. (1997). The VideoToolbox software for visual psychophysics: Transforming numbers into movies. *Spatial Vision, 10*(4), 437–442.

Pokorny, J., Smith, V. C., Verriest, G., & Pinckers, A. J. L. G. (1979). Congenital Color Defects. In J. Pokorny, V. C. Smith, G. Verriest, & A. J. L. G. Pinckers (Eds.), *Congenital and Acquired Color Vision Defects*. New York: Grune and Stratton.

Pugh, E. N., Jr, & Mollon, J. D. (1979). A theory of the Π1 and Π3 color mechanisms of Stiles. *Vision research, 19*, 293–312.

Regan, B. C., & Mollon, J. D. (1997). The relative salience of the cardinal axes of colour space in normal and anomalous trichromats. In C. R. Cavonius (Ed.), *Colour vision deficiencies XIII* (pp. 261–270). Dordrecht, The Netherlands: Kluwer Academic Publishers.

Rodriguez-Carmona, M. & Barbur, J. L. (2012). Variability in normal and defective colour vision: consequences for occupational environments. In Best, J. Colour Design. Elsevier Science and Technology.

Smith, V. C., Pokorny, J., & Sun, H. (2000). Chromatic contrast discrimination: Data and prediction for stimuli varying in L and M cone excitation. *Color Research and Application, 25*(2), 105–115.

Souza, G. S., Gomes, B. D., Lacerda, E. M. C. B., Saito, C. A., Filho, M. D. S., & Silveira, L. C. L. (2008). Amplitude of the Transient Visual Evoked Potential (tVEP) as a function of achromatic and chromatic contrast: Contribution of different visual pathways. *Visual neuroscience, 25*(3), 317–325.

Stockman, A., MacLeod, D. I. A., & Johnson, N. E. (1993). Spectral sensitivities of the human cones. *Journal of the Optical Society of America A, 10*(12), 2491. https://doi.org/10.1364/JOSAA.10.002491.

Tregillus, K. E. M., Isherwood, Z. J., Vanston, J. E., Engel, S. A., MacLeod, D. I. A., Kuriki, I., & Webster, M. A. (2021). Color compensation in anomalous trichromats assessed with fMRI. *Current Biology, 31*(5), 936–942.e4.

Vingrys, A. J., & Mahon, L. E. (1998). Color and luminance detection and discrimination asymmetries and interactions. *Vision Research, 38*(8), 1085–1095.

von der Twer, T., & MacLeod, D. I. A. (2001). Optimal nonlinear codes for the perception of natural colours. *Network: Computation in Neural Systems, 12*(3), 395–407.

Watanabe, A., Pokorny, J., & Smith, V. C. (1998). Red-green chromatic discrimination with variegated and homogenous stimuli. *Vision Research, 38*, 3271–3274.

Webster, M. A., Juricevic, I., & McDermott, K. C. (2010). Simulations of adaptation and color appearance in observers with varying spectral sensitivity. Ophthalmic and Physiological Optics, 30, 602–610.

Yeh, T., Pokorny, J., & Smith, V. C. (1993). Chromatic discrimination with variation in chromaticity and luminance: Data and theory. *Vision research, 33*(13), 1835–1845.

Yeh, T., Lee, B. B., & Kremers, J. (1995). Temporal response of ganglion cells of the macaque retina to cone-specific modulation. *Journal of the Optical Society of America A, 12*(3), 456. https://doi.org/10.1364/JOSAA.12.000456.